

# Removal Hg<sup>0</sup> from Flue Gas with Modified VTSS by KBr and KI

Yingjie Shi<sup>1,2\*</sup>, Yakui Li<sup>2</sup>

<sup>1</sup>China University of Mining & Technology, Beijing, China

<sup>2</sup>Chinese Research Academy of Environmental Sciences, Beijing, China

Email: <sup>\*</sup>shiaei@sina.com, 809761318@qq.com

Received 5 December 2015; accepted 10 December 2015; published 17 December 2015

---

## Abstract

Vanadium titanium steel slag (VTSS) containing transition metal can promote the adsorption of Hg<sup>0</sup>. The method of KBr and KI impregnation was applied to modify VTSS and the properties of the adsorbents were tested. The Hg<sup>0</sup> removal tests were carried out with a fixed bed under different conditions. The results showed that the Hg<sup>0</sup> adsorption capacity increase with the increasing temperature. The efficiency was highest with KI(3)/VTSS at 200°C and adsorption capacity was 163.4 ug/g after 3 h. The highest Hg<sup>0</sup> removal efficiency were 90.6% for KI(3)/VTSS, 73.5% for KBr(10)/VTSS/ VTSS at 120°C, respectively.

## Keywords

Hg<sup>0</sup>, Vanadium Titanium Steel Slag, KX, Capacity

---

## 1. Introduction

Mercury is a major atmospheric pollutant because of its toxicity and bioaccumulation in the food chains, which causes adverse effects on human health and environment. Coal-fired power plants are major sources for the atmospheric mercury pollution through the discharge of flue gas [1].

There are many technologies which can control the mercury emission from coal-fired plants, such as sorbent injection, coal washing, and simultaneous removal by the existing flue gas purification device. However, the removal of Hg<sup>0</sup> is more difficult due to its higher volatility, chemical inertness, and insolubility in water [2]. Activated carbon powder has been commercially used in the flue gas for the adsorption of mercury. But a large carbon/Hg ratio is required to achieve a high removal efficiency for mercury and the cost for activated carbon injection is great. Therefore, many researchers focused on low-cost sorbents [3]-[5].

In recent years, the modified sorbents have been tested to capture elemental mercury (Hg<sup>0</sup>) in flue gas. The bentonite modified by acid treatment and sulfur impregnation surface property was improved [6]. FA was commonly taken as an adsorbent for the capture of mercury and FA were found to enhance Hg<sup>0</sup> adsorption because of their significant catalytic effect [7] [8]. Clays and the modified clays have been used as adsorbents and catalyst supports for treating waste gas [9].

---

\*Corresponding author.

Vanadium-titanium steel slag (VTSS) is suitable for the application in mercury oxidation. Thus, in this study, the halide salts of KBr and KI were used to modify VTSS. Therefore, the characteristics of the  $\text{Hg}^0$  removal by KBr/VTSS and KI/VTSS in flue gas will be studied in this paper.

## 2. Experiments

### 2.1. Preparation of Sorbents

The adsorbents were prepared by impregnation method using VTSS, KBr and KI. The VTSS was collected from the converter slag of Panzhihua iron and steel Company. VTSS was washed with deionized water, dried at  $110^\circ\text{C}$  for 24 h and stored in a desiccator for future use. Halide-impregnated VTSS were prepared by an impregnation method using a mixed solution of KI or KBr and VTSS under vigorous stirring at room temperature for 3 h. The weight loading of KI or KBr was varied over the range of 1 - 10 wt% to the VTSS. The final sorbents were dried at  $100^\circ\text{C}$  for 12 h before test. The sorbents are denoted as KBr(x)/VTSS and KI(x)/VTSS, where x represents the weight ratio (%) of KBr or KI to VTSS.

### 2.2. Characterization of Sorbents

BET surface area was determined by the BET method using  $\text{N}_2$  adsorption-desorption isotherm, which was measured on a gas sorption analyzer (ThermoFisher, ESCALAB 250) at liquid nitrogen temperature. The BET surface area and pore volume significantly increased when KBr and KI was loaded on the VTSS. XRD pattern was recorded between  $5^\circ$  and  $80^\circ$  at a step of  $2^\circ \text{min}^{-1}$  by an X-ray diffractionmeter (Utimal III) with  $\text{Cu K}\alpha$  radiation (40 kV and 40 mA).

### 2.3. Sorbents Activity Test

A laboratory-scale fixed-bed apparatus was constructed, as shown in **Figure 1**, to explore activity of the prepared adsorbents. The setup included four parts: an elemental mercury permeation tube; a fixed-bed quartz reactor (12 mm i.d., 500 mm length) with a thermocouple to control temperature of the furnace; an online Lumex RA-915M Zeeman mercury analyzer, 3012H  $\text{SO}_2$  analyzer and a tail-end absorption equipment. A constant quantity of  $\text{Hg}^0$  vapor was supplied into the gas steam. The exhaust gas from the mercury analyzer was introduced into activated carbon before being expelled into the atmosphere. The reaction temperature is  $70^\circ\text{C}$ ,  $120^\circ\text{C}$ ,  $200^\circ\text{C}$ , respectively. For the tests, the  $\text{Hg}^0$  removal efficiency  $\eta(\%)$  and  $\text{Hg}^0$  adsorption capacity  $Q$  ( $\mu\text{g/g}$ ) were defined as (1) and (2), respectively:

$$\eta = (1 - \rho/\rho_0) \times 100\% \quad (1)$$

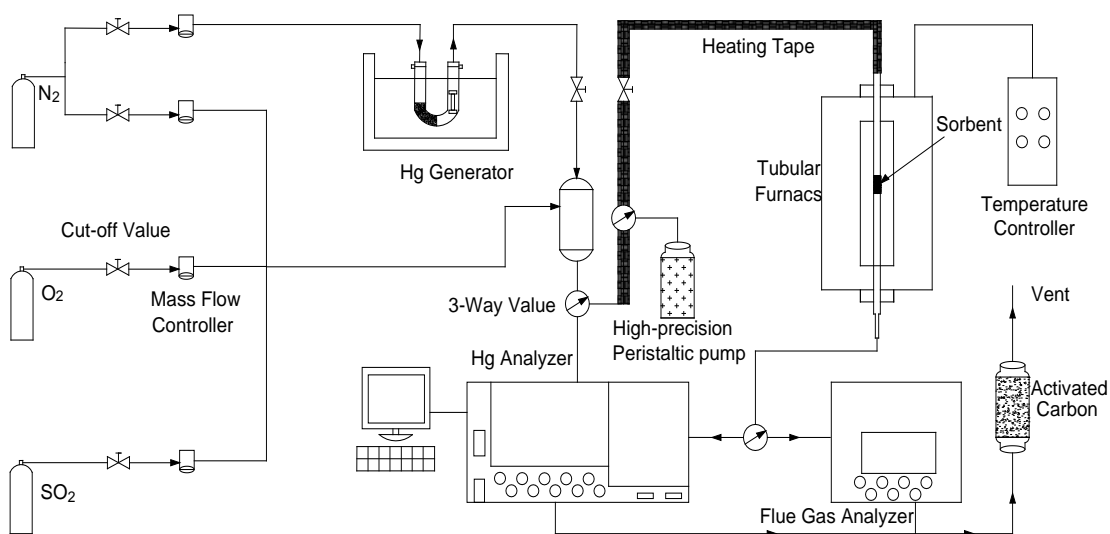


**Figure 1.** Schematic diagram of experimental system.

$$Q = \frac{1}{m} \left( \int_{t_0}^{t_1} (\rho_0 - \rho) \times f \times dt \right) \quad (2)$$

where  $\eta$  is mercury removal efficiency,  $f$  is the gas flow rate ( $\text{Nm}^3/\text{min}$ ),  $m$  is the mass of sorbent (g),  $\rho_0$  and  $\rho$  are the  $\text{Hg}^0$  concentrations at the inlet and outlet of the fixed-bed reactor, respectively, and  $t$  was the adsorption time.

### 3. Results and Discussion

#### 3.1. Characterization of Sorbents

##### 3.1.1. Scanning Electron Microscope

XRD patterns of the samples are given in **Figure 2**. From **Figure 2**, it can be seen that the main phases present in the raw VTSS were crystalline components, which were always present as the major phases in VTSS. And also, the most of the raw VTSS particles were irregular and only a few were spherical in shape. However, the surfaces of KBr and KI appeared to be spongy. It indicated that the surfaces of these large spheres had plenty of KBr and KI particles attached, which greatly enhanced surface roughness of the VTSS particles.

##### 3.1.2. XRD

XRD patterns of the samples are given in **Figure 3**. It can be seen that the main phases present in the raw VTSS were crystalline components, including tri-calcium silicate, Ca-Ti oxides and Ferromagnesian. In the KBr and KI doped VTSS samples, there was weak increase in intensity of the peaks attributed to KBr and KI.

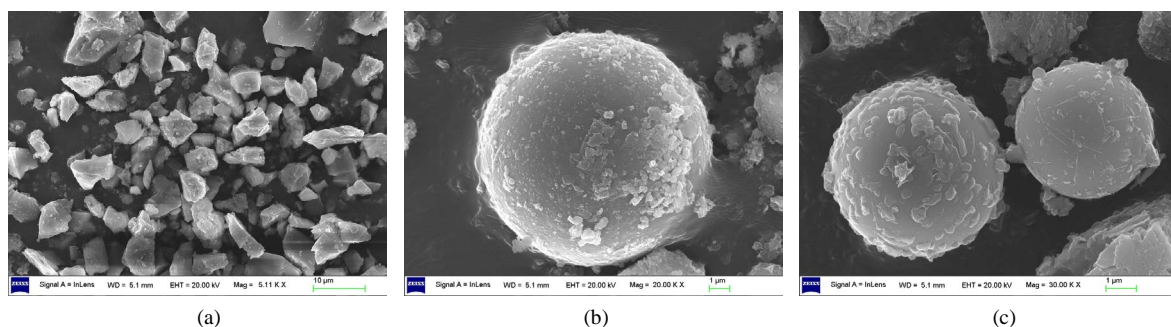


**Figure 2.** SEM images of the adsorbents: (a) VTSS; (b) KBr(3)/VTSS and (c) KI(3)/VTSS.

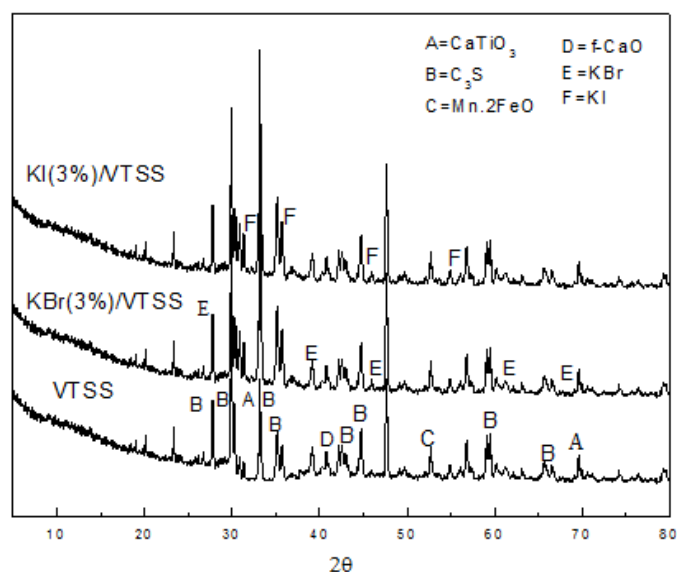


**Figure 3.** XRD images of the adsorbents VTSS, KBr(3)/VTSS and KI(3)/VTSS.

### 3.2. Sorbents Activity Test

#### 3.2.1. The effect of Adsorption Temperature

The effects of different adsorption temperatures (70°C, 120°C and 200°C) on the mercury adsorption capacity and Hg<sup>0</sup> removal efficiency for the KI/VTSS and KBr/VTSS are shown in **Figure 4** and **Figure 5**. **Figure 4** and **Figure 5** show that the Hg<sup>0</sup> removal efficiency of both KI/VTSS and KBr/VTSS increased with the rise of adsorption temperatures. The Hg<sup>0</sup> removal capacity for the KBr(10)/VTSS reached to 80.2 μg/g at 70°C, 114.1 μg/g at 120°C and 141.2 μg/g at 200°C in 3 h, respectively. For KI(3)/VTSS, the Hg<sup>0</sup> removal capacity reached to 116.4 μg/g at 70°C, 153.1 μg/g at 120°C and 163.4 μg/g at 200°C in 3 h, respectively.

The adsorption of Hg<sup>0</sup> on the surfaces of the materials can be typically classified into two types of processes: physisorption and chemisorption. Chemisorption is associated with a certain activation energy and proceeds at a limited rate which increases with rise in temperature. The clear enhancement in Hg<sup>0</sup> removal with temperature suggests that the removal of Hg<sup>0</sup> on these modified clays occurred mainly by chemisorption:



where X is Br, I.

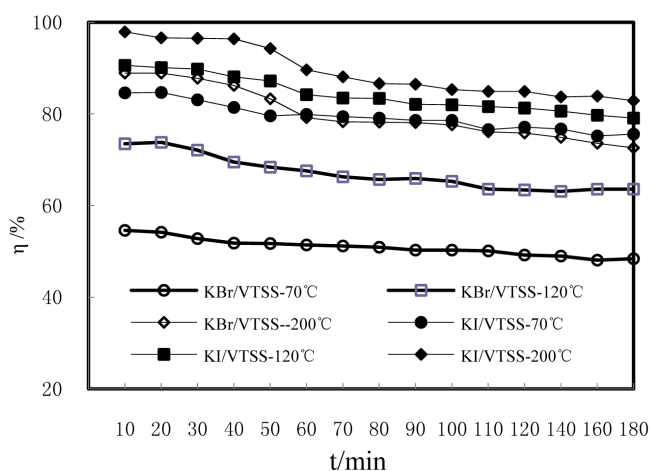


**Figure 4.** Effects of temperature on Hg<sup>0</sup> removal efficiency.

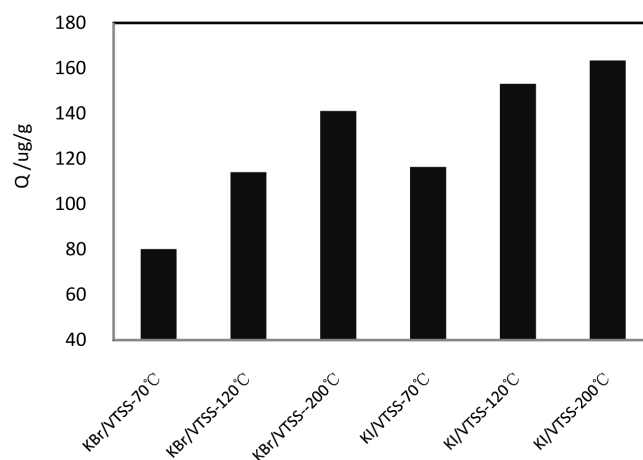


**Figure 5.** Effects of temperature on Hg<sup>0</sup> adsorption capacity.

### 3.2.2. The Effect of SO<sub>2</sub>

The effects of SO<sub>2</sub> on the Hg<sup>0</sup> removal were investigated in our study and the results are shown in **Figure 6** and **Figure 7**. It was observed that the introduction of SO<sub>2</sub> decreased the Hg<sup>0</sup> removal efficiency of the sorbents at 120°C. When 1480 mg/m<sup>3</sup> SO<sub>2</sub> was added, the mercury removal efficiency increased from 73.5% to 67.2% after 3 h for the KBr(10)/VTSS, from 90.6% to 79.1% after 3 h for the KI(3)/VTSS. However, the heavy inhibitive effect on mercury removal were observed When 3140 mg/m<sup>3</sup> SO<sub>2</sub> was added. The possible main reason was that SO<sub>2</sub> competed with Hg<sup>0</sup> for active sites on the KBr/VTSS or KI/VTSS so as to inhibit Hg<sup>0</sup> adsorption, which were necessary for the Hg<sup>0</sup> adsorption.

### 3.2.3. The Effect of O<sub>2</sub> on Hg<sup>0</sup> Removal

The effect of O<sub>2</sub> concentration on the Hg<sup>0</sup> adsorption capacity and Hg<sup>0</sup> removal efficiency were shown in **Figure 8** and **Figure 9**. The Hg<sup>0</sup> removal efficiency decreased from the initial 43.6% to 30.1% in the absence of O<sub>2</sub> over 3 h for the KBr(10)/VTSS, from 52.2% to 37.8% for the KBr(10)/VTSS at the same condition.

### 3.2.4. The Effect H<sub>2</sub>O on Hg<sup>0</sup> Removal

The effect of H<sub>2</sub>O concentration on the Hg<sup>0</sup> removal was shown in **Figure 10**. The Hg<sup>0</sup> removal efficiency decreased to 40.5% and 39.9% over 3 h for KBr(10)/VTSS and KI(3)/VTSS respectively when 4 vol.% was added. However, the efficiency decreased to 31.6% and 30.8% over 3 h for KBr(10)/VTSS and KI(3)/VTSS respectively when 8 vol.% was added. Two possible reasons were responsible for it. First, water vapor competed with Hg<sup>0</sup> for active sites and thus inhibited the Hg<sup>0</sup> adsorption. Secondly, the adsorbed water vapor may react with SO<sub>2</sub> to form sulfate, which would cover surface of the adsorbents and affect Hg<sup>0</sup> oxidation by deactivating the adsorbents to certain extent.

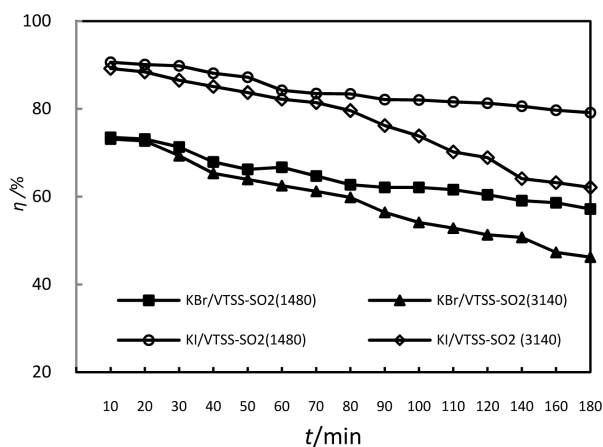


**Figure 6.** Effects of SO<sub>2</sub> on Hg<sup>0</sup> removal efficiency.

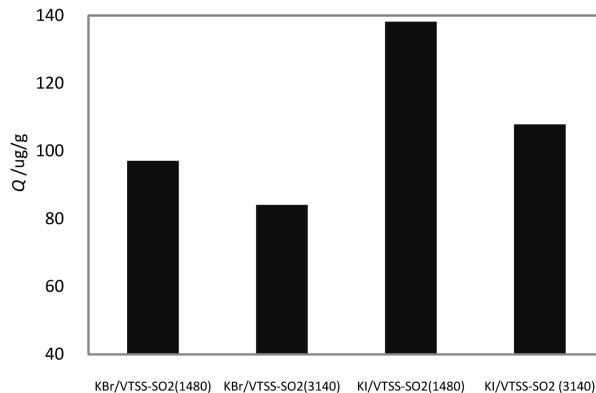


**Figure 7.** Effects of SO<sub>2</sub> on Hg<sup>0</sup> adsorption capacity.

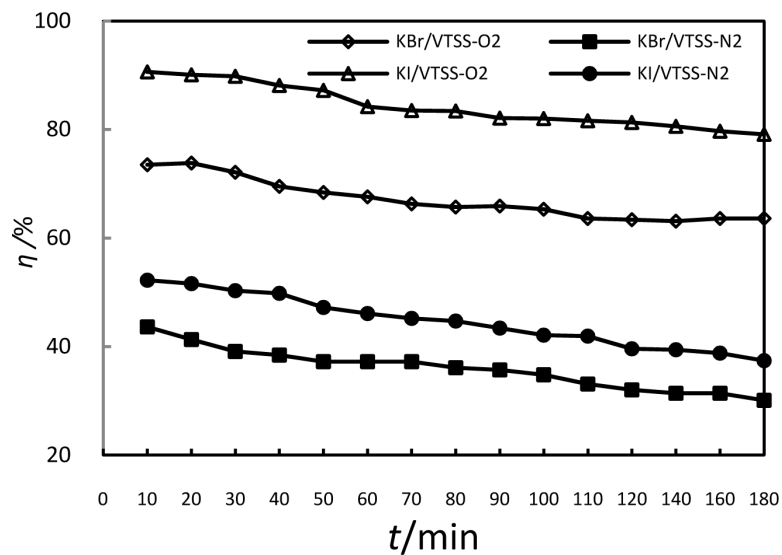


Figure 8. Effects of O<sub>2</sub> concentration on Hg<sup>0</sup> removal efficiency.

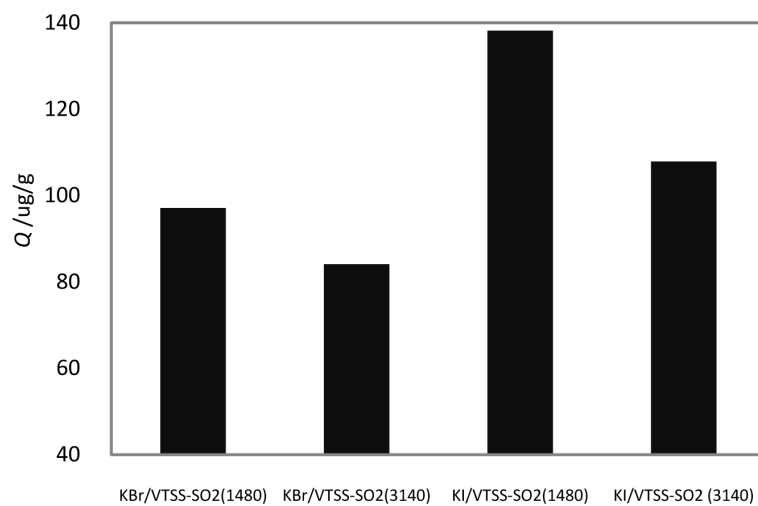


Figure 9. Effects of O<sub>2</sub> concentration on Hg<sup>0</sup> adsorption capacity.

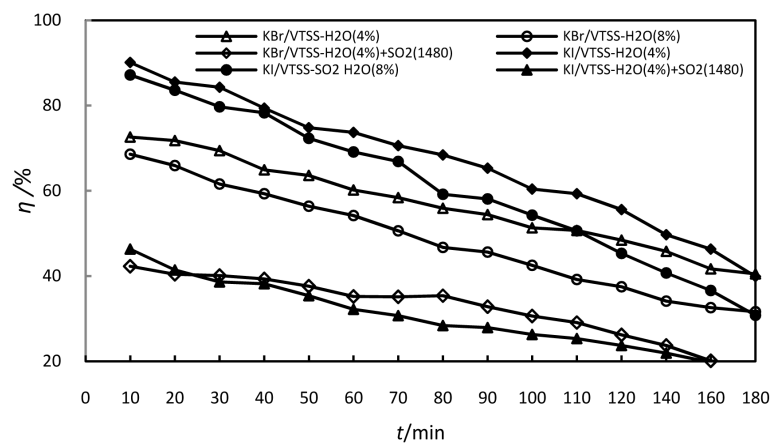


Figure 10. Effects of H<sub>2</sub>O on Hg<sup>0</sup> removal efficiency.

## 4. Conclusions

1) The results showed that the  $\text{Hg}^0$  adsorption efficiency and capacity increase with the increasing temperature. The efficiency was highest with adsorbents impregnated by 3% KI at 200°C, which was 97.9% and adsorption capacity was 163.4  $\mu\text{g/g}$  after 3 h.

2)  $\text{SO}_2$  and  $\text{H}_2\text{O}$  inhibited the  $\text{Hg}^0$  adsorption while  $\text{O}_2$  improved remarkably. The  $\text{Hg}^0$  removal efficiency increased with the increasing KBr and KI loading capacity.

3) The highest  $\text{Hg}^0$  removal efficiency were 73.5% and 90.6% respectively with sorbents impregnated by 10% KBr and 3% KI at 120°C, and adsorption capacity were 114.1 and 153.1  $\mu\text{g/g}$  after 3 h respectively.

## References

- [1] UNEP (2013) Global Mercury Assessment. UNEP Division of Technology, Industry and Economics, Chemicals Branch International Environment House, Geneva, 9-16.
- [2] Klasson, K.T., Lima, I.M. and Boihem, J.L.L. (2010) Feasibility of Mercury Removal from Simulated Flue Gas by Activated Chars Made from Poultry Manures. *J. Envir. Manag.*, **91**, 2466-2470. <http://dx.doi.org/10.1016/j.jenvman.2010.06.028>
- [3] De, M., Azargohar, R., Dalai, A.K. and Shewchuk, S.R. (2013) Mercury Removal by Bio-Char Based Modified Activated Carbons. *Fuel*, **103**, 570-578. <http://dx.doi.org/10.1016/j.fuel.2012.08.011>
- [4] Hocquel, M., Unerberger, S. and Hein, K.R.G. (2001) Influence of Temperature and HCl Concentration on Mercury Speciation in the Presence of Calcium Oxide (CaO). *Chem. Eng. Technol.*, **24**, 1267-1272. [http://dx.doi.org/10.1002/1521-4125\(200112\)24:12<1267::AID-CEAT1267>3.0.CO;2-Y](http://dx.doi.org/10.1002/1521-4125(200112)24:12<1267::AID-CEAT1267>3.0.CO;2-Y)
- [5] Bilirgen, H. and Romero, C. (2012) Mercury Capture by Boiler Modifications with Sub-Bituminous Coals. *Fuel*, **94**, 361-367. <http://dx.doi.org/10.1016/j.fuel.2011.10.047>
- [6] Kwons, S. and Vidic, R.D. (2000) Evaluation of Two Sulfur Impregnation Methods on Activated Carbon and Bentonite for the Production of Elemental Mercury Sorbents. *Environ. Eng. Sci.*, **17**, 303-313. <http://dx.doi.org/10.1089/ees.2000.17.303>
- [7] Dunham, G.E. and DeWall, R.A. (2003) Fixed-Bed Studies of the Interactions between Mercury and Coal Combustion Fly Ash. *Fuel Process. Technol.*, **82**, 197-213. [http://dx.doi.org/10.1016/S0378-3820\(03\)00070-5](http://dx.doi.org/10.1016/S0378-3820(03)00070-5)
- [8] Galbreath, K.C., Zygarlicke, C.J., Toman, D.L. and Tibbetts, J.E. (2004) Effects of  $\text{NO}_x$ ,  $\alpha\text{-Fe}_2\text{O}_3$ , and  $\gamma\text{-Fe}_2\text{O}_3$  on Mercury Transformations in a 7-kW Coal Combustion System. *Fuel Process. Technol.*, **86**, 429-448. <http://dx.doi.org/10.1016/j.fuproc.2004.03.003>
- [9] Assebban, M., Kasmi, A.E., Harti, S. and Chafik, T. (2015) Intrinsic Catalytic Properties of Extruded Clay Honeycomb Monolith toward Complete Oxidation of Air Pollutants. *J. Hazard. Mater.*, **300**, 590-597.